J. Mod. Power Syst. Clean Energy (2019) 7(6):1721–1734
https://doi.org/10.1007/s40565-019-0530-9

Investment optimization of grid-scale energy storage for supporting different wind power utilization levels

Yunhao LI[1], Jianxue WANG[1], Chenjia GU[1], Jinshan LIU[2], Zhengxi LI[2]

Abstract With the large-scale integration of renewable generation, energy storage system (ESS) is increasingly regarded as a promising technology to provide sufficient flexibility for the safe and stable operation of power systems under uncertainty. This paper focuses on grid-scale ESS planning problems in transmission-constrained power systems considering uncertainties of wind power and load. A scenario-based chance-constrained ESS planning approach is proposed to address the joint planning of multiple technologies of ESS. Specifically, the chance constraints on wind curtailment are designed to ensure a certain level of wind power utilization for each wind farm in planning decision-making. Then, an easy-to-implement variant of Benders decomposition (BD) algorithm is developed to solve the resulting mixed integer nonlinear programming problem. Our case studies on an IEEE test system indicate that the proposed approach can co-optimize multiple types of ESSs and provide flexible planning schemes to achieve the economic utilization of wind power. In addition, the proposed BD algorithm can improve the computational efficiency in solving this kind of chance-constrained problems.

Keywords Wind power, Capacity investment, Energy storage, Power system planning, Chance constraint

CrossCheck date: 13 February 2019

Received: 21 September 2018 / Accepted: 13 February 2019 / Published online: 23 May 2019

✉ Jianxue WANG
jxwang@mail.xjtu.edu.cn

Yunhao LI
yhli_ee@126.com

Chenjia GU
809679595@qq.com

Jinshan LIU
js-clark@163.com

Zhengxi LI
18209783306@163.com

[1] School of Electrical Engineering, Xi'an Jiaotong University, Xi'an 710049, China

[2] State Grid Qinghai Electric Power Company, Xi'ning 810000, China

1 Introduction

Nowadays, many countries are committed to promoting the development of renewable power generation to cope with global warming and fossil energy crisis. As reported in [1], China pledged to prioritize renewable generation and reach the non-fossil energy target of 20% by 2030. Nevertheless, owing to the natural intermittency and stochastic volatility of renewable energy, the utilization of renewable generation, especially centralized wind power generation, is still technically difficult. Reference [2] mentions that in China, the annual wind curtailment in 2012 has exceeded 20 GWh, which accounted for 17% of all the available wind power. It is urgent to integrate and consume wind power safely and economically.

As far as the wind curtailment issue is concerned, power systems should have sufficient flexibility to mitigate short-term fluctuations of wind power as well as the temporal mismatch between wind power and load. With the increasingly mature energy storage technology, grid-scale ESS is regarded as a potential solution to provide the required flexibility for accommodating large-scale wind power generation [3]. The related grid applications of ESSs include, but are not limited to: peak shaving, power

balancing and system upgrade deferral [4]. However, considering the high capital cost of ESS, installing large-capacity ESSs for such applications may lead to poor investment economy [5]. Hence, it requires an optimization-based ESS planning method to ensure that the ESS investment is reasonable and economic for improving wind power utilization.

To date, researchers have shown an increasing interest in grid-scale ESS planning problems in power systems with wind power integration. A deterministic planning model is proposed in [6] to investigate the optimal sizing of ESS for renewable power plants with a well-designed storage operation strategy. To smooth the net load variations, reference [7] presents a fast sizing method for battery energy storage (BES) based on calculating specific battery-sizing indices. In [8], the ESS sizing model is further augmented by incorporating the system peak-shaving policies. The above studies focus on the optimal sizing of ESS in a single-bus model that assumes the transmission capacity to be unlimited. To further consider the role of ESS in transmission congestion relief, plenty of methods have been proposed for the joint optimization of ESS sizing and siting in transmission-constrained networks. According to the way of promoting wind power utilization, we categorize these methods into the following three types.

1) Price-guidance methods. References [9, 10] propose a market-based optimal power flow framework to optimize the sizing and siting of compressed air energy storage (CAES) considering different wind penetration levels. Reference [11] incorporates the unit commitment problem into the ESS planning and designs a near-optimal solution strategy. This type of research makes use of the price advantage of wind power, that is, due to the low marginal price, the wind power can be utilized preferentially to minimize the total cost of meeting the load demand.
2) Robust-oriented methods. Reference [12] proposes a scenario tree-based stochastic programming model for CAES planning considering nonanticipative operating behaviors. In [13, 14], the impacts of uncertain wind power on the voltage profiles, transmission congestion costs are respectively considered in ESS planning problems by using the AC power flow model. All these models [12–14] are formulated to cater for the full utilization of available wind power. In addition, robust optimization has also been well adopted in ESS planning studies [15, 16] to obtain robust solutions that can ensure reliable system operation without any wind curtailment under uncertainties.
3) Penalty-based methods. Reference [17] provides a practical and feasible ESS planning method for realistic large-scale systems. Reference [18] introduces specific constraints to guarantee a certain level of profitability in ESS investment. In [19], a dynamic programming model is presented to address the multi-stage impacts of uncertainties on the investment of BES. What the above studies [17–19] have in common is that they penalize the wind curtailment as one of the optimization objectives to enhance wind power utilization.

All the three types of models above for minimizing wind curtailment can provide reasonable ESS planning decisions that ensure high utilization of wind power. However, few of these studies pay attention to the conflict between wind power utilization and ESS investment economy. We believe that the level of wind power utilization will have a significant impact on ESS investment costs. The problem which motivates this paper is the need for flexible ESS planning models that support the precise adjustment of wind power utilization level and help decision makers achieve a desired trade-off.

On the other hand, different technologies of energy storage have significantly different operation characteristics and cost-effectiveness performances. Reference [20] indicates that there is no single ideal storage technology that can well satisfy the needs of power systems for power and energy services. Therefore, how to determine the optimal storage portfolio for the reliable and economic operation of power systems is also a critical problem when various storage technologies are available. Reference [21] designs both analytical and optimization-based frameworks for joint sizing of multiple storage technologies based on the predetermined net load profiles. Reference [22] further considers transmission constraints and proposes a storage portfolio optimization method under a deterministic environment. So far, however, there has been little discussion about the non-deterministic storage portfolio optimization problem with full consideration of wind power uncertainties.

In light of the above issues, this paper proposes a flexible transmission-constrained ESS planning approach considering uncertain wind power and load. To precisely control the wind power utilization level, specific chance constraints are formulated on the occurrence probability and amount of curtailing wind power generation for each wind farm. Then we establish a scenario-based chance-constrained programming model that supports the non-deterministic optimization of storage portfolio. The resulting nonlinear nonconvex problem is reformulated using a proper relaxation process and is solved by a customized variant of Benders decomposition (BD) algorithm. Finally, case studies on a modified IEEE-24 system are presented to validate the proposed method.

The main contributions of this paper are threefold: ① A scenario-based chance-constrained model is proposed to achieve flexible adjustment of the risk level of wind power curtailment and the wind power utilization rate in the ESS planning under uncertainty; ② In addition to consideration of wind power uncertainties, the modeling of storage portfolio problem takes into account a number of factors that reflect differences between different storage technologies, including the lifetime, the investment costs per unit power/energy capacity, the typical energy/power ratio of energy storage and the storage loss during the charging and discharging; ③ According to the problem structure, a modified BD algorithm is developed to improve the computational efficiency of solving this kind of chance-constrained programming problem. Detailed techno-economic analysis for ESS planning is provided considering different energy storage portfolios and wind power utilization levels.

The remainder of this paper is organized as follows. Section 2 introduces the mathematical formulation of the chance-constrained ESS planning problem. Section 3 gives the BD type solution method. Case studies are given and discussed in Section 4. Then Section 5 concludes this paper.

2 Problem formulation

This paper concentrates on the static ESS planning problem driven by uncertain load and wind power generation. As with the classical stochastic ESS studies [9–12], this paper employs stochastic programming to model the above uncertainties by using a finite set of scenarios. Note that both the wind power output and wind power fluctuation have peak distribution characteristics, that is, a high level of wind power output or wind power variability only occurs in small probability. Since a typical stochastic programming model generally considers every scenario in the scenario pool, ESSs should be built to cater for the peak wind power output or mitigate the high-level wind power volatility, which may result in costly and inefficient planning schemes. To avoid overinvestment in ESS, this paper extends conventional ESS planning models by adding scenario-based chance constraints on wind power utilization, where a proper amount of wind curtailment is allowed over the planning period. The detailed problem formulation is given below.

2.1 Scenario reduction

Considering that for multiple uncertainties, it is easier to obtain their scenario information than the specific probability distribution, we adopt the scenario-based method to characterize multiple uncertainties by discrete scenarios. The scenarios defined in this paper are composed of the daily time series of load and wind power. In the real-world applications, the raw scenario set can be obtained with the historical load and wind speed data. Given that it is computationally intractable to deal with large numbers of scenarios in the optimization model, a clustering-based scenario reduction method is proposed here to generate a representative scenario set from the raw scenario set.

For simplicity, the daily net load time series is employed to reflect the uncertain characteristic of each scenario. Then, to implement the clustering analysis, the similarity degree D_{ij} between every two scenarios is evaluated by:

$$D_{ij} = D_{ij}^{E} \frac{\sqrt{\left(\sum_{t=1}^{|\Gamma|} L_{it}^2\right)\left(\sum_{t=1}^{|\Gamma|} L_{jt}^2\right)}}{\sum_{t=1}^{|\Gamma|} L_{it} L_{jt}} \tag{1}$$

where L_{it} and L_{jt} are the net load values in period t of scenario i and j; Γ is the set of time periods; and D_{ij}^{E} denotes the Euclidean distance between scenarios i and j. Note that in addition to the Euclidean distance, this paper also introduces the cosine distance to measure the similarity of the net load fluctuation between time-series scenarios.

A clustering method called density peaks clustering (DPC) [23] is then adopted to divide the raw scenario set into several clusters. Compared with traditional clustering techniques, DPC is more suitable for the actual time series dataset because it can determine the optimal cluster number. Through clustering analysis, the scenarios with similar daily net load shapes will be assigned to the same cluster, then we can intuitively produce a representative scenario set by sampling few scenarios in each cluster. In addition, to ensure the effectiveness of scenario reduction, we carry out the scenario sampling and determine the weight coefficient of each scenario by solving an optimization problem of minimizing the Kantorovich distance between the raw scenario set and the reduced scenario set, a detailed description of which can be found in [24].

2.2 Mathematic formulation

2.2.1 Constraints at planning level

Given that the capacity investment of ESS has a discrete nature in reality, this paper provides a mixed integer formulation to achieve discrete planning decisions with multiple storage technologies. An integer decision variable n_i^q represents the number of energy storage units of technology q built at bus i, which is subject to:

$$0 \le n_i^q U^q \le u_i^q \quad \forall i \in \Omega, q \in H \tag{2}$$

$$\sum_{i\in\Omega} n_i^q U^q \le u_S^q \quad \forall q \in H \tag{3}$$

where U^q is the per-unit energy capacity of storage technology q; u_i^q and u_S^q are the maximum allowable investment capacities of storage technology q built at bus i and in the entire system, respectively; and Ω and H are the bus set and storage technology set, respectively.

Constraints (2) and (3) limit the number of energy storage units built at the local and system-wide levels. In addition, the value of parameter u_i^q can be artificially set to reflect the geographic location restrictions of some storage technologies, such as pumped hydro energy storage (PHES) and CAES.

2.2.2 Constraints at operational level

In this paper, a daily time planning horizon is adopted to model the operational behavior of power systems as well as ESSs under uncertainties. Since we mainly focus on the benefits of ESS for the adjustment of active power, a DC network model is adopted to keep the formulation simple. The uncertain wind power and load are considered by using the reduced scenario set. Detailed constraints of the daily operation model are given as follows.

1) DC power flow constraints.

$$F_{ijk}(t)=B_{ij}(\theta_{ik}(t)-\theta_{jk}(t)) \quad \forall ij \in \Phi, k \in \Psi, t \in \Gamma \tag{4}$$

$$F_{ij,\min} \le F_{ijk}(t) \le F_{ij,\max} \quad \forall ij \in \Phi, k \in \Psi, t \in \Gamma \tag{5}$$

$$-\pi \le \theta_{ik}(t) \le \pi \quad \forall i \in \Omega, k \in \Psi, t \in \Gamma \tag{6}$$

$$\theta_{ik}(t)= 0 \quad i = i_s, \forall k \in \Psi, t \in \Gamma \tag{7}$$

$$\begin{aligned} P_{ik}^G(t) + P_{ik}^W(t) + \sum_{q\in H} P_{SD,ik}^q(t) = P_{ik}^L(t) + \sum_{q\in H} P_{SC,ik}^q(t) \\ + P_{ik}^{CW}(t) + \sum_{j\in O_i} F_{ijk}(t) \quad \forall i \in \Omega, k \in \Psi, t \in \Gamma \end{aligned} \tag{8}$$

where the subscript k is the k^{th} scenario (the same below); $F_{ijk}(t)$ is the power flow along line i-j in period t; $F_{ij,\min}$ and $F_{ij,\max}$ are the corresponding lower and upper bounds; B_{ij} is the susceptance of line i-j; $\theta_{ik}(t)$ and $\theta_{jk}(t)$ are the voltage angles at bus i and j in period t, respectively; i_s denotes the slack bus number; $P_{ik}^G(t)$ and $P_{ik}^{CW}(t)$ are the conventional generator output and wind curtailment at bus i in period t, respectively; $P_{ik}^W(t)$ and $P_{ik}^L(t)$ are both input parameters, which denote the wind power and load at bus i in period t, respectively; $P_{SD,ik}^q(t)$ and $P_{SC,ik}^q(t)$ are the discharging and charging power of storage technology q at bust i in period t; Φ and Ψ are the sets of transmission lines and reduced scenarios, respectively; and O_i is the set of buses connected to bus i by available transmission lines.

Constraint (4) represents the DC power flow relationship. Constraints (5)-(7) define the operation limits for the line power flow and nodal angle. Constraint (8) is the nodal power balance equation.

2) Operational constraints for conventional generators. In this study, the quadratic fuel cost function of the conventional generator is approximated by a piecewise linearization. Specifically, the generator output $PG_{ik}(t)$ is divided into l linear segments, each of which is subject to:

$$P_{ik}^G(t) = P_{i,\min}^G + \sum_{\alpha=1}^{l} P_{ik}^{G,\alpha}(t) \quad \forall i \in \Omega, k \in \Psi, t \in \Gamma \tag{9}$$

$$0 \le P_{ik}^{G,\alpha}(t) \le P_{i,\max}^{G,\alpha} \quad \forall i \in \Omega, k \in \Psi, t \in \Gamma, \alpha \in [1, l] \tag{10}$$

where $P_{ik}^{G,\alpha}(t)$ is the α^{th} segment of the generator output $P_{ik}^G(t)$; $P_{i,\max}^{G,\alpha}$ is the corresponding upper bound; and $P_{i,\min}^G$ is the minimum output of the conventional generator at bus i.

In addition, the generator output $P_{ik}^G(t)$ in each period is restricted by the generation ramp-rate limitation:

$$-R_i \le P_{ik}^G(t+1) - P_{ik}^G(t) \le R_i \quad \forall i \in \Omega, k \in \Psi, t \le |\Gamma| - 1 \tag{11}$$

where R_i is the maximum up/down ramp rate of the conventional generator at bus i.

3) Operational constraints for ESS. Firstly, the charging/discharging power is restricted by the power rating of ESS as follows:

$$0 \le P_{SD,ik}^q(t) \le n_i^q \gamma_{D,ik}^q(t) \cdot U^q / T^q \tag{12}$$

$$0 \le P_{SC,ik}^q(t) \le n_i^q \gamma_{C,ik}^q(t) \cdot U^q / T^q \tag{13}$$

$$\begin{cases} \gamma_{D,ik}^q(t)+\gamma_{C,ik}^q(t) \le 1 \\ \gamma_{D,ik}^q(t) \in \{0,1\} \\ \gamma_{C,ik}^q(t) \in \{0,1\} \end{cases} \tag{14}$$

where $\forall i \in \Omega; k \in \Psi; q \in H; t \in \Gamma$; $\gamma_{D,ik}^q(t)$ and $\gamma_{C,ik}^q(t)$ are two binary decision variables that determine whether the energy storage units built at bus i operate in discharging or charging state in period t; T^q is the rated discharge duration of storage technology q, which represents the typical energy/power ratio in its practical application. Note that by introducing parameters U^q and T^q, we can, to a certain extent, take into account the investment and application

characteristics of different storage technologies in the ESS planning modeling.

Furthermore, the energy capacity limits, which is related to the charging/discharging power, are given as below:

$$0 \le S_{ik}^{q}(t) \le n_i^q U^q \quad \forall i \in \Omega, k \in \Psi, q \in H, t \in \Gamma \tag{15}$$

$$S_{ik}^{q}(t=1) = S_{ik}^{q}(t=|\Gamma|) \quad \forall i \in \Omega, k \in \Psi, q \in H \tag{16}$$

$$S_{ik}^{q}(t+1) - S_{ik}^{q}(t) = \eta_C^q P_{SC,ik}^{q}(t) - \frac{1}{\eta_D^q} P_{SD,ik}^{q}(t) \quad \forall i \in \Omega, k \in \Psi, q \in H, t \le |\Gamma| - 1 \tag{17}$$

where S_{ik}^{q} is the state of charge (SoC) of storage technology q at bus i in period t; η_C^q and η_D^q are the charging and discharging efficiencies of storage technology q, respectively. Constraint (15) makes the SoC less than the rated energy capacity. Constraint (16) describes the coupling relationship between the charging/discharging power and SoC. To satisfy the daily continuous operation of ESS, constraint (17) makes sure that the SoC in the last period should be the same with its initial condition.

2.2.3 Constraints on wind curtailment

Firstly, the wind curtailment should be no more than the actual available wind power, which can be expressed by:

$$0 \le P_{ik}^{CW}(t) \le P_{ik}^{W}(t) \quad \forall i \in \Omega, k \in \Psi, t \in \Gamma \tag{18}$$

Furthermore, to guarantee a certain level of wind power utilization for each wind farm, this paper introduces a chance constraint as shown in (19), which restricts the occurrence probability of excessive wind curtailment within a certain risk tolerance level ε:

$$\Pr\left\{\sum_{t\in\Gamma} P_i^{CW}(t) \le (1-\kappa)\sum_{t\in\Gamma} P_i^{W}(t)\right\} \ge 1-\varepsilon \quad \forall i \in \Omega \tag{19}$$

where κ represents the utilization rate of wind power that needs to be satisfied.

On the basis of the reduced scenario set, constraint (19) is further reformulated into the following constraints:

$$\left[\sum_{t\in\Gamma} P_{ik}^{CW}(t) - (1-\kappa)\sum_{t\in\Gamma} P_{ik}^{W}(t)\right](1-z_k) \le 0 \quad \forall i \in \Omega, k \in \Psi \tag{20}$$

$$\sum_{k\in\Psi} z_k p_k \le \varepsilon \quad z_k \in \{0,1\} \tag{21}$$

where z_k is a binary decision variable; p_k is the occurrence probability of scenario k. For scenario k, it can be observed that z_k is used as an indicator to determine whether the wind power can be curtailed over the predefined range ($z_k = 1$) or not ($z_k = 0$). More importantly, note that the values of κ and ε can be flexibly adjusted to reflect different needs of planning decision makers for the wind power utilization level. Accordingly, an effective trade-off between wind curtailment and ESS investment costs can be studied in the ESS planning.

2.2.4 Objective function

The above constraints indicate that a feasible planning scheme should be able to ensure the safe system operation without load shedding and excessive wind curtailment. Aiming at finding the least-cost planning solution, this paper defines the objective function V as the minimization of both the planning-stage cost and the weighted operational-stage cost, which is given by:

$$V = \min\left[C_{Cap} + C_F + \sum_{k\in\Psi} p_k\left(C_{V,k} + C_{G,k} + C_{L,k}\right)\right] \tag{22}$$

Specifically, the first element in (22) is the daily investment cost of all storage units, which is formulated by:

$$C_{Cap} = \frac{1}{365}\sum_{i\in\Omega}\sum_{q\in H}\gamma^q\left(c_E^q n_i^q U^q + c_P^q n_i^q \cdot U^q/T^q\right) \tag{23}$$

where γ^q is the capital recovery factor of storage technology q; c_E^q and c_P^q are the investment costs corresponding to the energy rating and power rating of storage technology q, respectively.

The second element is the daily fixed ESS operation & maintenance (O&M) cost, which is defined as follows [12]:

$$C_F = \sum_{i\in\Omega}\sum_{q\in H} c_F^q n_i^q \cdot U^q/T^q \tag{24}$$

where c_F^q denotes the daily fixed O&M cost corresponding to the power rating of storage technology q. Note that the fixed ESS O&M cost is only related to the installed ESS power capacity.

The third element is the daily variable ESS O&M cost, which is formulated as follows [12]:

$$C_{V,k} = \sum_{i\in\Omega}\sum_{q\in H}\sum_{t\in\Gamma} P_{SD,ik}^{q}(t) c_V^q \quad \forall k \in \Psi \tag{25}$$

where c_V^q denotes the variable O&M cost of storage technology q. It can be observed that the value of $C_{V,k}$ depends on the daily operation of all storage units.

The fourth element is the daily generator fuel cost approximated by piecewise linearization, which is given by [15]:

$$C_{G,k} = \sum_{i\in\Omega}\sum_{t\in\Gamma}\left(c_{G,i}^0 + \sum_{\alpha=1}^{l} c_{G,i}^{\alpha} P_{ik}^{G,\alpha}(t)\right) \quad \forall k \in \Psi \tag{26}$$

where $c^0_{G,i}$ is the fixed cost of the generator at bus i corresponding to its minimum output; $c^{\alpha}_{G,i}$ denotes the linearized cost parameter for the generator output over segment α at bus i.

The last element is the daily ESS loss cost, which is defined as follows:

$$C_{L,k} = c_L \sum_{i\in\Omega}\sum_{q\in H}\sum_{t\in\Gamma}\left[P^q_{SD,ik}(t)(1-\eta^q_D)/\eta^q_D + P^q_{SC,ik}(t)\left(1-\eta^q_C\right)\right] \quad \forall k \in \Psi \tag{27}$$

where c_L is the penalty cost of storage loss during charging and discharging. Note that the storage loss during the daily operation, which is also an undesirable waste of energy like the wind curtailment, is rarely considered in the previous studies. Since different storage technologies have significant differences in the charging/discharging efficiency, it is necessary to introduce the corresponding loss cost into the objective function so as to take into account the impact of the charging/discharging efficiency on storage portfolio optimization.

Due to the existence of bilinear terms in (12), (13) and (20), the proposed ESS planning model is a complicated mixed integer nonlinear programming (MINLP) problem. In Section 3, a solution method inspired by the bilinear BD algorithm [25] is presented to solve this chance-constrained problem.

3 Solution method

3.1 Linear formulation of original MINLP problem

Firstly, we note that the introduction of the variable O&M cost and ESS loss cost in the objective function (22) can already help avoid the simultaneous charging and discharging of ESS. Hence, for the non-convex constraints (12) and (13), this paper relaxes them by taking the convex hull of the corresponding feasible region, which is given by:

$$\begin{cases} P^q_{SD,ik}(t) + P^q_{SC,ik}(t) \le n^q_i \cdot U^q/T^q \quad P^q_{SD,ik}(t) \ge 0 \\ P^q_{SC,ik}(t) \ge 0 \quad \forall i \in \Omega, k \in \Psi, q \in H, t \in \Gamma \end{cases} \tag{28}$$

Obviously, by replacing (12) and (13) with (28), a total of $2|\Omega||H||\Psi||\Gamma|$ binary decision variables can also be removed to reduce the problem-solving scale.

In addition, for the bilinear constraint (20), we adopt the McCormick linearization method [26] to obtain its linear counterpart as follows:

$$\sum_{t\in\Gamma} P^{CW}_{ik}(t) - \sum_{t\in\Gamma} P^{CW'}_{ik}(t) - (1-z_k)(1-\kappa)\sum_{t\in\Gamma} P^{W}_{ik}(t) \le 0 \quad \forall i \in \Omega, k \in \Psi \tag{29}$$

$$\begin{cases} P^{CW}_{ik}(t) - P^{W}_{ik}(t)(1-z_k) \le P^{CW'}_{ik}(t) \le P^{CW}_{ik}(t) \\ \qquad\qquad \forall i \in \Omega, k \in \Psi, t \in \Gamma \\ 0 \le P^{CW'}_{ik}(t) \le P^{W}_{ik}(t) z_k \quad \forall i \in \Omega, k \in \Psi, t \in \Gamma \end{cases} \tag{30}$$

where $P^{CW'}_{ik}(t)$ is the auxiliary variable that replaces the bilinear term $P^{CW}_{ik}(t)z_k$. It can be observed that (29) and (30) are completely equivalent to (20) because the desired restriction on wind curtailment also only works under the responsive scenarios (z_k=0).

Using the above relaxation, the original ESS planning model is reformulated into a mixed integer linear programming (MILP) model. However, it is still a challenge to directly solve this problem due to the multiple scenarios. Given that its computational complexity can be decentralized by decomposing the two-stage problems with respect to each scenario, a BD type solution method is presented in the following.

3.2 Modified BD algorithm

According to the general BD framework [27], the proposed ESS planning problem can be decomposed into an investment master problem and a series of operation subproblems over the reduced scenario set.

3.2.1 Operation subproblems

The operation subproblems are employed to check whether the first-stage decision obtained in the master problem is global optimal. They come in two forms, which depends upon the values of binary decision variables z_k. Consider the fixed decision variables $\hat{n}^{q(m)}_i$ and $\hat{z}^{(m)}_k$ obtained in the m^{th} BD iteration, the subproblem for the responsive scenario ($\hat{z}^{(m)}_k = 0$) is formulated as (31), subject to (4)–(7), (9)–(11), (15)–(18), (25)–(28) and (32)–(34).

$$\varphi^{(m)}_k = \min\left[C_{V,k} + C_{G,k} + C_{L,k} + M\left(\sum_{i\in\Omega}\eta^1_{ik} + \sum_{i\in\Omega}\sum_{t\in\Gamma}\eta^2_{ik}(t)\right)\right] \tag{31}$$

$$\sum_{t\in\Gamma} P^{CW}_{ik}(t) \le (1-\gamma_\kappa)\sum_{t\in\Gamma} P^{W}_{ik}(t) + \eta^1_{ik} \quad \forall i \in \Omega \tag{32}$$

$$P_{ik}^{G}(t)+P_{ik}^{W}(t)+\sum_{q\in H}P_{SD,ik}^{q}(t)=P_{ik}^{L}(t)-\eta_{ik}^{2}(t)+\sum_{q\in H}P_{SC,ik}^{q}(t)+P_{ik}^{CW}(t)+\sum_{j\in O_i}F_{ijk}(t)\quad\forall i\in\Omega,t\in\Gamma \tag{33}$$

$$n_i^q=\hat{n}_i^{q(m)}\quad\forall i\in\Omega,q\in H \tag{34}$$

where the objective function $\varphi_k^{(m)}$ aims to minimize the operational-stage cost under the responsive scenario; n_{ik}^1 and $n_{ik}^2(t)$ are two non-negative slack variables for the wind curtailment and load, respectively; M is a penalty coefficient to penalize n_{ik}^1 and $n_{ik}^2(t)$ in (31). These two slack variables are employed to ensure that such subproblems are always solvable, thus giving an optimality cut as below:

$$\left[\hat{\varphi}_k^{(m)}+\sum_{i\in\Omega}\sum_{q\in H}\tau_{ik}^{q(m)}\left(n_i^q-\hat{n}_i^{q(m)}\right)\right](1-z_k)\le\xi_k \tag{35}$$

where $\tau_{ik}^{q(m)}$ is the dual multiplier associated with (34); ξ_k is the system operation cost during the second stage. Note that the indicator z_k is employed to ensure that the bilinear cut (35) is active only when $z_k=0$.

For the non-responsive scenario $\hat{z}_k^{(m)}=1$, another optimality subproblem, which has a similar formulation to the previous one, is given by:

$$\psi_k^{(m)}=\min\left(C_{V,k}+C_{G,k}+C_{L,k}+M\sum_{i\in\Omega}\sum_{t\in\Gamma}\eta_{ik}^{2}(t)\right) \tag{36}$$

Equation (26) is subject to (4)-(7), (9)-(11), (15)-(18), (25)-(28), (33) and (34). Note that this subproblem only penalizes the load shedding. Likewise, a corresponding bilinear optimality cut is formulated as follows:

$$\left[\hat{\psi}_k^{(m)}+\sum_{i\in\Omega}\sum_{q\in H}v_{ik}^{q(m)}\left(n_i^q-\hat{n}_i^{q(m)}\right)\right]z_k\le\xi_k \tag{37}$$

where $v_{ik}^{q(m)}$ is the dual multiplier of (34) with respect to the latter subproblem.

Although the bilinear terms in (35) and (37) can be linearized by the McCormick method, the unavoidable introduction of auxiliary variables and constraints will increase the computational burden of the master problem. This study therefore develops another linearized counterpart of this kind of bilinear optimality cuts.

Here we take the optimality cut (35) as an example. Consider a set $E=\{(i,q):i\in\Omega,q\in\mathrm{H}\}$, we can obtain a specific subset $E_1^{(m)}=\left\{(i,q)\in E:\tau_{ik}^{q(m)}\ge 0\right\}$ and its complimentary set $E_2^{(m)}=\left\{(i,q)\in E:\tau_{ik}^{q(m)}<0\right\}$ under scenario k in the m^{th} BD iteration. Here we define an auxiliary parameter $\zeta_k^{1(m)}$ as follows:

$$\zeta_k^{1(m)}=\sum_{(i,q)\in E_1^{(m)}}\tau_{ik}^{q(m)}n_{i,\max}^q+\sum_{(i,q)\in E_2^{(m)}}\tau_{ik}^{q(m)}n_{i,\min}^q \tag{38}$$

where $n_{i,\max}^q$ and $n_{i,\min}^q$ are respectively the physical upper and lower bounds of n_i^q. Then, a valid linear formulation of the optimality cut (35) is given below:

$$\left(\hat{\varphi}_k^{(m)}-\sum_{i\in\Omega}\sum_{q\in H}\tau_{ik}^{q(m)}\hat{n}_i^{q(m)}\right)(1-z_k)+\sum_{i\in\Omega}\sum_{q\in H}\tau_{ik}^{q(m)}n_i^q-\zeta_k^{1(m)}z_k\le\xi_k \tag{39}$$

Remark We mention that when $z_k=0$, it is clear that cut (39) reduces to a traditional Benders cut, which is valid for any feasible solution (n_i^q, $z_k=0$). When $z_k=1$, the left side of the reduced cut should have:

$$\sum_{i\in\Omega}\sum_{q\in H}\tau_{ik}^{q(m)}n_i^q-\zeta_k^{1(m)}\le\max_{n_i^q}\sum_{i\in\Omega}\sum_{q\in H}\tau_{ik}^{q(m)}n_i^q-\zeta_k^{1(m)}=0\le\xi_k \tag{40}$$

which also indicates that the reduced cut is valid for any feasible solution (n_i^q, $z_k=1$), thus proving the validity of the proposed cut (39). It can be further observed that, by introducing parameter $\zeta_k^{1(m)}$, cut (39) is not only inherently linear without adding auxiliary variables or constraints, but also avoids excessive relaxation of (35). As the upper/lower bounds of decision variables n_i^q are naturally available, it is feasible to perform this linearization in practice.

Similarly, for another optimality cut (37), we can also formulate its linearized counterpart as follows:

$$\left(\hat{\psi}_k^{(m)}-\sum_{i\in\Omega}\sum_{q\in H}v_{ik}^{q(m)}\hat{n}_i^{q(m)}\right)z_k+\sum_{i\in\Omega}\sum_{q\in H}v_{ik}^{q(m)}n_i^q-\zeta_k^{2(m)}(1-z_k)\le\xi_k \tag{41}$$

where parameter $\zeta_k^{2(m)}$ is obtained according to the values of $v_{ik}^{q(m)}$ as well as the upper/lower bound of n_i^q.

3.2.2 *Investment master problem*

The master problem aims to minimize the total cost under the planning constraints and the optimality cuts passed by subproblems. According to (39) and (41), the master problem in the m^{th} iteration can be written as a MILP problem in the following:

$$V^{(m)} = \min\left(C_{Cap} + C_F + \sum_{k\in\Psi} p_k \xi_k\right) \tag{42}$$

It is subject to (2), (3), (21), (23), (24), (43) and (44). Equations (43) and (44) can be solved by using commercial MILP solvers.

$$\left(\hat{\varphi}_k^{(l)} - \sum_{i\in\Omega}\sum_{q\in H} \tau_{ik}^{q(l)} \hat{n}_i^{q(l)}\right)(1 - z_k) + \sum_{i\in\Omega}\sum_{q\in H} \tau_{ik}^{q(l)} n_i^q - \zeta_k^{1(l)} z_k \le \xi_k \quad \forall k \in \Psi, l \le m-1 \tag{43}$$

$$\left(\hat{\varphi}_k^{(l)} - \sum_{i\in\Omega}\sum_{q\in H} \tau_{ik}^{q(l)} \hat{n}_i^{q(l)}\right)(1 - z_k) + \sum_{i\in\Omega}\sum_{q\in H} \tau_{ik}^{q(l)} n_i^q - \zeta_k^{1(l)} z_k \le \xi_k \quad \forall k \in \Psi, l \le m-1 \tag{44}$$

On the basis of the above master problem and subproblems, the proposed ESS planning problem can be solved using a conventional iterative solution procedure [27]. The flow chart is presented in Fig.1.

4 Case study

In this section, a modified IEEE 24-bus system is studied to validate the proposed ESS planning approach. The network topology is shown in Fig. 2.

The time horizon is 24 hours in time steps of 1 hour. A reduced scenario set consisting of 55 scenarios is selected from the historical data of load and wind power output. According to the ideas of [15, 22], the original IEEE 24-bus system is modified in the following three aspects:

1) To render the test system less reliable and aggravate the transmission congestion, all the loads are assumed to be 1.3 times of the original values, and capacities of all transmission lines are reduced by 20%. The ramp-rate limitations are also imposed on the conventional generators.
2) Five wind farms, each with a capacity of 250 MW, 250 MW, 250 MW, 550 MW and 550 MW, are added to buses 1, 4, 5, 14 and 17, respectively. The penetration level of wind generation with respect to the overall load is 49.93%.
3) Three different storage technologies, PHES, CAES and BES, are considered in the case studies. For each storage technology, the energy capacity per unit is set to 1000 MWh, 400 MWh and 40 MWh, respectively, and the rated discharge duration is set to 10 hours, 8

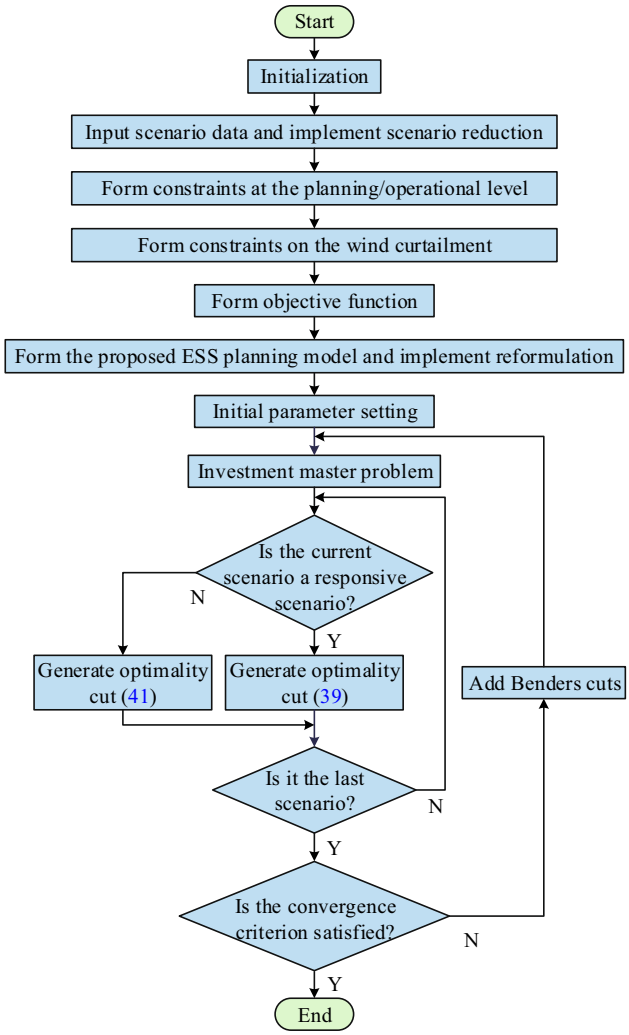

Fig. 1 Flow chart of proposed ESS planning methodology

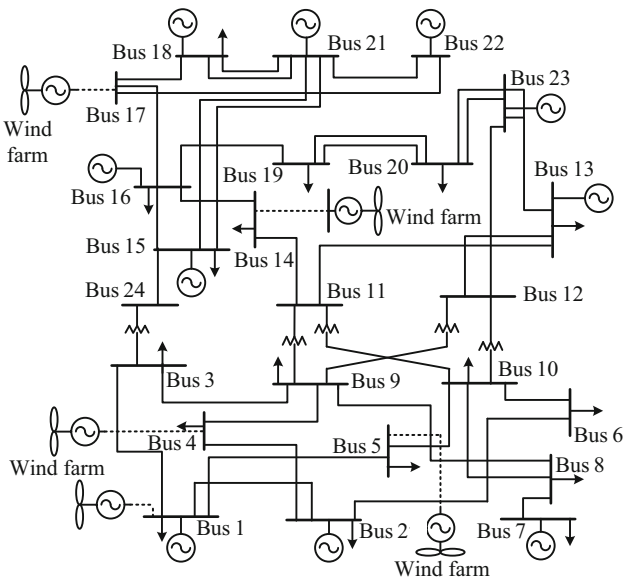

Fig. 2 Single line diagram of modified IEEE 24-bus system

Table 1 ESS planning results with single storage technology

Case	Planning scheme	Daily cost ($ per day)				Total cost ($ per day)
		Investment cost	O&M cost	Fuel cost	ESS loss cost	
R1	PHES (300 MW/3000 MWh): n_3=100 MW/1000 MWh, n_{22}=200 MW/2000 MWh	253538	4562	1050374	26017	1334491
R2	CAES (300 MW/2400 MWh): n_7=50 MW/400 MWh, n_{22}=250 MW/2000 MWh	239049	4553	1066982	29551	1340135
R3	BES (500 MW/1000 MWh): n_6=120 MW/240 MWh, n_8=60 MW/120 MWh, n_{10}=60 MW/120 MWh, n_{16}=60 MW/120 MWh, n_{17}=200 MW/400 MWh	231202	9926	1072301	8703	1322132

hours and 2 hours, respectively. Detailed parameter setting can be found in [28].

4.1 Experiments with different storage technologies

This subsection aims to show the effect of different storage technologies on planning decisions through comparison. Three cases, each of which considers only one storage technology, are defined as follows:

1) Case R1 only considers PHES, and the site locations are limited to buses 3, 7, and 22 to reflect geographic restrictions.
2) Case R2 only considers CAES while the site locations are the same as those in C1.
3) Case R3 only considers BES, and the site locations are limited to buses 6, 8, 10, 16 and 17, which are selected based on the most congested lines.

With the risk level ε and wind utilization rate κ set to 10% and 95%, Table 1 gives the planning results for cases R1-R3, where n_i in each scheme denotes the power/energy capacity planned to be installed in bus i. It can be clearly seen that the features of each storage technology have a direct impact on planning results. Specifically, since BES has the minimum energy capacity per unit and can be built more flexibly than PHES and CAES, the overall energy capacity built in case R3 is only 1000 MWh, which is 66.67% and 58.33% less than that in cases R1 an R2, respectively. However, the small energy/power ratio of BES also results in building a huge power capacity up to 500 MW in case R3, which is 1.67 times higher than that in cases R1 and R2. On the other hand, it can be observed that the planning scheme with larger energy capacity brings in more cost savings in terms of fuel costs, and the usage of BES is of salient benefit in reducing the ESS loss costs because of its high charging/discharging efficiency.

Two operation indices, which are respectively called the energy capacity utilization level (ECUL) and the power capacity utilization level (PCUL), are presented as follows to show how much the overall energy/power capacity is utilized during the daily/hourly system operation.

$$ECUL_k^q = \frac{\max\limits_{t\in\Gamma}\sum\limits_{i\in\Omega} S_{ik}^q(t) - \min\limits_{t\in\Gamma}\sum\limits_{i\in\Omega} S_{ik}^q(t)}{\sum\limits_{i\in\Omega} n_i^q U^q} \tag{45}$$

$$PCUL_k^q(t) = \frac{\max\left(\sum\limits_{i\in\Omega} P_{SD,ik}^q(t), \sum\limits_{i\in\Omega} P_{SC,ik}^q(t)\right)}{\sum\limits_{i\in\Omega} n_i^q \cdot U^q/T^q} \tag{46}$$

By calculating these two indices over the reduced scenario set, we obtain the statistical distribution characteristics of ESS utilization for cases R1-R3 as shown in Fig. 3.

Obviously, in terms of energy capacity, case R3 fully utilizes the built BESs in almost all scenarios, whereas the maximum ECUL in cases R1 and R2 are no larger than 80%, which means the corresponding built energy capacity has already exceeded the system operation requirements. On the other hand, cases R1 and R2 make better use of the built power capacity than case R3 in which the PCUL is less than 60% in a probability of 93.97%. It can be

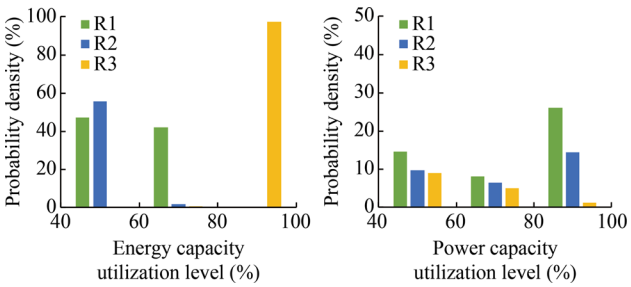

Fig. 3 Histogram for ESS utilization under cases R1-R3

Table 2 ESS planning results with two storage technologies

Case	Planning scheme	Daily cost ($ per day)				Total cost ($ per day)
		Investment cost	O&M cost	Fuel cost	ESS loss cost	
R4	PHES+CAES (300 MW/2800 MWh): PHES: n_{22}=200 MW/2000 MWh; CAES: n_{22}=100 MW/800 MWh	248708	4297	1055031	25382	1333418
R5	PHES+BES (400 MW/1600 MWh): PHES: n_{22}=100 MW/1000 MWh; BES: n_6=20 MW/40 MWh, n_8=20 MW/40 MWh n_{10}=60 MW/120 MWh, n_{17}=200 MW/400 MWh	223233	7482	1063501	14283	1308499
R6	CAES+BES (350 MW/1600 MWh): CAES: n_3=100 MW/800 MWh, n_{22}=50 MW/400 MWh; BES: n_{10}=20 MW/40 MWh, n_{17}=180 MW/360 MWh	212005	6313	1071247	19052	1308617

observed that the power capacity built in case R3 is over-invested because the power regulation requirements are also met in cases R1 and R2 with less power capacity. Therefore, under such circumstance, the main driving factor of PHES and CAES construction is the demand for power service, while that of BES construction is the demand for energy service. The above discussion demonstrates that in the ESS planning, using only one type of ESS can hardly meet the unstructured demand for power and energy capacity of system operation without redundant capacity investments.

4.2 Experiments with different storage technology portfolios

In this subsection, with the same parameter settings, we obtain all possible joint planning schemes (R4-R7) by enumerating each storage technology portfolio. Note that cases R4-R6 in Table 2 correspond to the joint planning schemes with only two storage technologies, while case R7 in Table 3 introduces all three storage technologies.

As indicated in Tables 2 and 3, all planning schemes (R4-R7) involving multiple storage technologies cost less than the previous schemes (R1-R3) in terms of the total cost. In particular, case R7, which introduces all three storage technologies, has the minimum total cost among cases R1-R7, thus revealing the effectiveness and necessity of the joint planning of various types of energy storage. Furthermore, it can be seen that although the investment cost of case R7 is larger than that of case R6, the cost savings in the remaining three types of costs still render case R7 the most economic planning scheme. Actually, there is no clear positive or inverse relationship between the above four types of costs, it is therefore necessary to introduce all of them as optimization objectives in the ESS planning model.

Figure 4 further shows simulation results of system operation before/after building ESS (case R7). It can be observed that all three types of energy storage are involved in storing wind energy during the valley-load period and drastically promote wind power utilization by peak shaving. In addition, BES also provides the capability of power regulation to maintain power balance at the 9th, 10th and 15th hours.

Likewise, we employ the above two indices to investigate the changes in ESS utilization after introducing multiple storage technologies. Taking case R7 as an example, the utilization of each storage technology is analyzed and depicted in Fig. 5. It can be seen that, compared to the separate use of each storage technology, the combined use of three storage technologies in case R7 effectively improves the utilization level of all types of energy storage. Specifically, in terms of power capacity for PHES, CAES and BES, the probability of PCUL above 80% significantly increases from 26.01%, 14.39% and 1.12% to 40.16%, 26.27% and 6.41%. On the other hand, the redundant investment in the energy capacity of PHES and CAES is also alleviated, where the probability of ECUL above 60% correspondingly increases from 42.1% and 1.55% to 49.87% and 16.71%, respectively.

As a conclusion, compared with cases R1-R3, case R7 takes better advantage of the low-cost energy capacity of PHES and CAES as well as the low-cost power capacity of BES, thus providing a more reasonable planning scheme.

4.3 Additional analyses

4.3.1 Impact of ESS loss cost

In order to investigate whether it is necessary to involve the energy loss of ESS in the ESS planning studies, two planning schemes (R8 and R9) are obtained with the same

Table 3 ESS planning results with all three storage technologies

Case	Planning scheme	Daily cost ($ per day)				Total cost ($ per day)
		Investment cost	O&M cost	Fuel cost	ESS loss cost	
R7	PHES+CAES+BES (350 MW/1800 MWh): PHES: n_3=100 MW/1000 MWh; CAES: n_{22}=50 MW/400 MWh; BES: n_{10}=20 MW/40 MWh, n_{17}=180 MW/360 MWh	216835	6216	1064369	17654	1305074

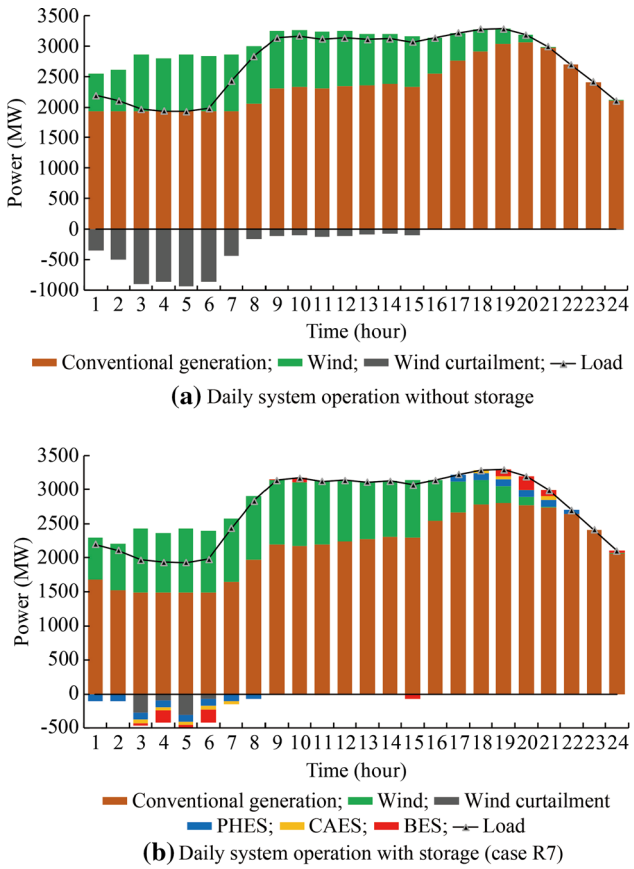

Fig. 4 Simulation results for daily system operation

parameter settings as cases R4 and R5, but ignoring the ESS loss cost in the objective function. Table 4 shows that compared to cases R4 and R5, more storage units with lower charge/discharge efficiency are built in cases R8 and R9 whereas high-efficiency storage units are removed. Specifically, the ESS loss costs of cases R8 and R9 increase by 85.09% and 69.41%, respectively, which is the main reason that results in more costly planning schemes. It can be concluded that the consideration of ESS loss cost can help to avoid unreasonable capacity investments of the storage technologies with low charging/discharging efficiency.

4.3.2 *Sensitivity analysis*

To analyze the conflict between the wind power utilization level and ESS investment decision, we take case R6 as the benchmark and obtain four other planning schemes as shown in Table 5 with the same storage portfolio but different values of ε and κ. Here we additionally calculate the penalty cost of wind curtailment in each case to reflect the impact of changes in wind power utilization level on the actual wind curtailment loss.

Table 5 indicates that owing to the restrictive requirements for wind power utilization, the storage investment costs in cases R10 and R12 are respectively increased by 17.12% and 27.5% as compared with the benchmark (case R6). However, the cost savings corresponding to wind curtailment reduction are quite limited because of the peak distribution characteristics of wind power, which leads to poor economy in cases R10 and R12. On the contrary, with an appropriate decrease in the wind power utilization level, less storage devices are required to be built in cases R11 and R13 whereas the corresponding wind curtailment costs slightly increase, thus the total cost is effectively reduced.

The above observations show that: ① the proposed chance-constrained approach can flexibly adjust the wind power utilization level in the ESS planning, thus helping decision-makers to better determine the most suitable planning scheme; ② blindly maximizing the wind power utilization does not necessarily help to improve the

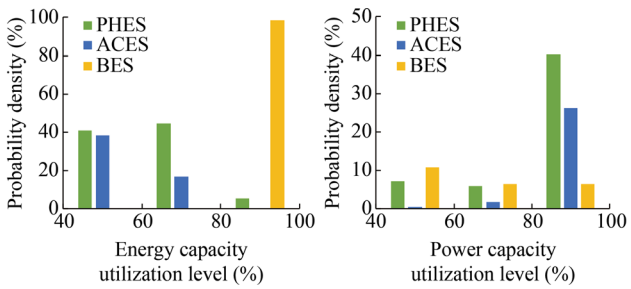

Fig. 5 Histogram for ESS utilization under case R7

Table 4 ESS planning results without considering ESS loss cost

Case	Planning scheme	Daily cost ($ per day)				Total cost ($ per day)
		Investment cost	O&M cost	Fuel cost	ESS loss cost (post evaluation)	
R8	PHES+CAES (300 MW/2800 MWh): PHES: n_{22}=200 MW/2000 MWh; CAES: n_{22}=100 MW/800 MWh	239049	6157	1056082	46981	1348269
R9	PHES+BES (320 MW/2240 MWh): PHES: n_{22}=200 MW/2000 MWh; BES: n_{10}=20 MW/40 MWh, n_{17}=100 MW/200 MWh	224513	5619	1057107	24197	1311436

Table 5 ESS planning results under different wind power utilization levels

κ (%)	ε (%)	Planning scheme	Daily cost ($ per day)				Curtailment cost ($ per day)	Total cost ($ per day)
			Investment cost	O&M cost	Fuel cost	Loss cost		
95.0	10.0	R6 (350 MW/1600 MWh): CAES: n_3=100 MW/800 MWh, n_{22}=50 MW/400 MWh; BES: n_{10}=20 MW/40 MWh, n_{17}=180 MW/360 MWh	212005	6313	1071247	19052	60247	1368864
95.0	7.5	R10 (320 MW/2440 MWh): CAES: n_3=100 MW/800 MWh, n_{22}=200 MW/1600 MWh; BES: n_{17}=20 MW/40 MWh	248297	4987	1065873	30213	52867	1402237
95.0	12.5	R11 (260 MW/1120 MWh): CAES: n_{22}=100 MW/800 MWh; BES: n_6=20 MW/40 MWh, n_{17}=140 MW/280 MWh	153668	4795	1096793	13634	66551	1335441
97.5	10.0	R12 (440 MW/2080 MWh): CAES: n_3=200 MW/1600 MWh; BES: n_{10}=60 MW/120 MWh, n_{17}=180 MW/360 MWh	270343	7639	1066263	22260	49326	1415831
92.5	10.0	R13 (230 MW/1360 MWh): CAES: n_3=50 MW/400 MWh, n_{22}=100 MW/800 MWh; BES: n_{10}=20 MW/40 MWh, n_{17}=60 MW/120 MWh	156517	4041	1083196	17934	71089	1332777

overall economy of power systems. Instead, the economy of system planning and operation can be improved by allowing the wind curtailment in an appropriate proportion.

4.3.3 Computational performance

Comparative experiments are carried out here to validate the proposed BD algorithm. In the solving procedure, all the above planning cases R1-R13 are solved by using CPLEX and the proposed BD algorithm, respectively. The relative optimality gap is set to 10^{-3} when using CPLEX, while the BD tolerance is also set to 10^{-3}. Comparison results of the computational performance are given in Table 6.

It can be observed that the proposed BD algorithm performs faster than the commercial solver CPLEX in all experiments. Specifically, the computational time by the BD algorithm is reduced by more than 80% in 11 of the

Table 6 Computational performance

Case	Solution time (s)	
	BD	CPLEX
R1	117.32	426.74
R2	111.46	627.31
R3	164.31	4684.77
R4	385.79	2618.99
R5	1771.23	27219.41
R6	1171.76	9441.81
R7	3498.11	19747.82
R8	320.64	4971.80
R9	1643.93	9731.70
R10	1579.53	5334.36
R11	716.44	5112.57
R12	1039.03	8623.44
R13	410.04	6282.77

above cases. Note that the subproblems are independent of each other, the solution efficiency of the BD algorithm can be further improved by parallel computing techniques.

5 Conclusion

This paper presents a chance-constrained ESS planning approach under uncertainty. A density-based clustering method is employed to generate a reduced scenario set to represent uncertain wind power and load. A scenario-based stochastic ESS planning model is established to achieve the joint planning of different energy storage technologies in transmission-constrained networks, and specific chance constraints are designed to ensure a certain level of wind power utilization. Numerical results in a modified IEEE 24-bus system indicate that: ① the planning schemes based on co-optimizing different storage technologies are more reasonable and economically efficient; ② more than 5.9% savings can be achieved in terms of the total cost by allowing a proper amount of wind curtailment; ③ the proposed BD algorithm performs at least 70% faster than using CPLEX to directly solve this kind of chance-constrained problems.

Although employing ESS can help defer the transmission construction, the economic relationship between the construction of ESSs and transmission lines is still ambiguous and needs to be further investigated. In the future, more efforts will be made to carry out the multi-stage co-planning of ESS and transmission network.

Acknowledgment This work was supported by National Key Research and Development Program of China (No. 2017YFB0902200) and the Science and Technology Project of State Grid Corporation of China (No. 5228001700CW).

References

[1] White House (2015) The United States and China issue joint presidential statement on climate change with new domestic policy commitments and a common vision for an ambitious global climate agreement in Paris. https://www.whitehouse.gov/the-press-office/2015/09/25/fact-sheet-united-states-and-china-issue-joint-presidential-statement. Accessed 18 September 2018

[2] Luo G, Li Y, Tang W et al (2016) Wind curtailment of China's wind power operation: evolution, causes and solutions. Renew Sustain Energy Rev 53:1190–1201

[3] Denholm P, Hand M (2011) Grid flexibility and storage required to achieve very high penetration of variable renewable electricity. Energy Policy 39(3):1817–1830

[4] Castillo A, Gayme DF (2014) Grid-scale energy storage applications in renewable energy integration: a survey. Energy Convers Manag 87:885–894

[5] Vargas LS, Bustos-Turu G, Larraín F (2015) Wind power curtailment and energy storage in transmission congestion management considering power plants ramp rates. IEEE Trans Power Syst 30(5):2498–2506

[6] Berrada A, Loudiyi K (2016) Operation, sizing, and economic evaluation of storage for solar and wind power plants. Renew Sustain Energy Rev 59:1117–1129

[7] Masaud TM, Oyebanjo O, Sen PK (2017) Sizing of large-scale battery storage for off-grid wind power plant considering a flexible wind supply-demand balance. IET Renew Power Gener 11(13):1625–1632

[8] Dong J, Gao F, Guan X et al (2017) Storage sizing with peak-shaving policy for wind farm based on cyclic Markov chain model. IEEE Trans Sustain Energy 8(3):978–989

[9] Ghofrani M, Arabali A, Etezadi-Amoli M et al (2013) Energy storage application for performance enhancement of wind integration. IEEE Trans Power Syst 28(4):4803–4811

[10] Ghofrani M, Arabali A, Etezadi-Amoli M et al (2013) A framework for optimal placement of energy storage units within a power system with high wind penetration. IEEE Trans Sustain Energy 4(2):434–442

[11] Pandžić H, Wang Y, Qiu T et al (2015) Near-optimal method for siting and sizing of distributed storage in a transmission network. IEEE Trans Power Syst 30(5):2288–2300

[12] Xiong P, Singh C (2016) Optimal planning of storage in power systems integrated with wind power generation. IEEE Trans Sustain Energy 7(1):232–240

[13] Wen S, Lan H, Fu Q et al (2015) Economic allocation for energy storage system considering wind power distribution. IEEE Trans Power Syst 30(2):644–652

[14] Hemmati R, Saboori H, Jirdehi MA (2017) Stochastic planning and scheduling of energy storage systems for congestion management in electric power systems including renewable energy resources. Energy 133:380–387

[15] Jabr RA, Džafić I, Pal BC (2015) Robust optimization of storage investment on transmission networks. IEEE Trans Power Syst 30(1):531–539
[16] Han X, Liao S, Ai X et al (2017) Determining the minimal power capacity of energy storage to accommodate renewable generation. Energies 10(4):1–17
[17] Fernández-Blanco R, Dvorkin Y, Xu B et al (2017) Optimal energy storage siting and sizing: a WECC case study. IEEE Trans Sustain Energy 8(2):733–743
[18] Xu B, Wang Y, Dvorkin Y et al (2017) Scalable planning for energy storage in energy and reserve markets. IEEE Trans Power Syst 32(6):4515–4527
[19] Qiu T, Xu B, Wang Y et al (2017) Stochastic multistage coplanning of transmission expansion and energy storage. IEEE Trans Power Syst 32(1):643–651
[20] Haas J, Cebulla F, Cao K et al (2017) Challenges and trends of energy storage expansion planning for flexibility provision in low-carbon power systems: a review. Renew Sustain Energy Rev 80:603–619
[21] Belderbos A, Virag A, D'haeseleer W et al (2017) Considerations on the need for electricity storage requirements: power versus energy. Energy Convers Manag 143:137–149
[22] Wogrin S, Gayme DF (2015) Optimizing storage siting, sizing, and technology portfolios in transmission-constrained networks. IEEE Trans Power Syst 30(6):3304–3313
[23] Rodriguez A, Laio A (2014) Clustering by fast search and find of density peaks. Science 344(6191):1492–1496
[24] Löhndorf N (2016) An empirical analysis of scenario generation methods for stochastic optimization. Eur J Oper Res 255(1):121–132
[25] Zhang Y, Wang J, Zeng B et al (2017) Chance-constrained two-stage unit commitment under uncertain load and wind power output using bilinear benders decomposition. IEEE Trans Power Syst 32(5):3637–3647
[26] McCormick GP (1976) Computability of global solutions to factorable nonconvex programs: part I—convex underestimating problems. Math Program 10(1):147–175
[27] Conejo AJ, Castillo E, Minguez R et al (2006) Decomposition techniques in mathematical programming: engineering and science applications. Springer, Berlin
[28] Zakeri B, Syri S (2015) Electrical energy storage systems: a comparative life cycle cost analysis. Renew Sustain Energy Rev 42:569–596

Yunhao Li received the B.S. degree in electrical engineering from Huazhong University of Science and Technology, China, in 2012. He is currently pursuing the Ph.D. degree at Xi'an Jiaotong University, China. His research interests include renewable energy and power system planning.

Jianxue Wang received the B.S., M.S., and Ph.D. degrees in electrical engineering from Xi'an Jiaotong University, China, in 1999, 2002, and 2006, respectively. He is currently a Professor in the School of Electrical Engineering, Xi'an Jiaotong University. His current research interests include microgrid planning and schdeuling, power system planning and scheduling, and electricity market.

Chenjia Gu received the B.S. degree from the School of Electrical Engineering, Xi'an Jiaotong University, China, in 2017. He is currently working toward the Ph.D. degree at Xi'an Jiaotong University. His major research interests include power system optimization and renewable energy/energy storage integration.

Jinshan Liu received the B.S. degree from Shenyang University of Technology, China, and the M.S. degree from Northeast Electric Power University, China. He has been engaged in research work in power system operation and control since joining the work.

Zhengxi Li received the B.S. degree from Shanghai Jiao Tong University, China, and the M.S. degree from Chongqing University, China. He has been engaged in research work in photovoltaic field since joining the work.